RESEARCH-ARTICLE

PixBric: Precision Morphological Control of Pre-Stretched Fabrics Through Tessellated Primitive Geometries

HYE JUN YOUN

JUN KYU CHOE

SOOYEON AHN

MARCELLO TANIA

SERENA XIN WEI SARA

HIROSHI ISHII

Published: 07 March 2026

TEI '26: Twentieth International Conference on Tangible, Embedded, and Embodied Interaction
March 8 - 11, 2026
IL, Chicago, USA

Conference Sponsors:
SIGCHI

TEI '26: Proceedings of the Twentieth International Conference on Tangible, Embedded, and Embodied Interaction (March 2026)
https://doi.org/10.1145/3731459.3773316
ISBN: 9798400718687

PixBric: Precision Morphological Control of Pre-Stretched Fabrics Through Tessellated Primitive Geometries

Hye Jun Youn
MIT Media Lab
Cambridge, USA
hyoun95@mit.edu

Jun Kyu Choe
MIT Media Lab
Cambridge, USA
juneq@mit.edu

SooYeon Ahn
Department of AI Convergence
Gwangju Institute of Science and Technology
Gwangju, Republic of Korea
syahn1160@gm.gist.ac.kr

Marcello Tania
MIT Media Lab
Cambridge, USA
m.cellotania@gmail.com

Serena Xin Wei Sara
MIT MechE
Cambridge, USA
sxsara@mit.edu

Hiroshi Ishii
MIT Media Lab
Cambridge, USA
ishii@media.mit.edu

Abstract

3D printing onto pre-stretched fabrics has emerged as a promising technique for fabricating self-shaping textiles. However, resulting morphing behaviors are often dictated by heuristics or arbitrarily selected parameters. We present *PixBric*, a pixel-based design framework that enables precise morphological control through tessellated primitive geometries printed onto biaxially stretched fabrics. Upon release, these units buckle into programmed 3D forms including undulations, curling, and bistable snapping. PixBric integrates parametric modeling, mechanical simulation, and empirical evaluation to map geometric parameters to deformation outcomes. We demonstrate applications spanning morphable typography, wearable rings, and reconfigurable surfaces. PixBric bridges digital simulation (*tide*) with the mechanical constraints of elastic substrates (*tied*), transforming complex material behaviors into accessible tools for learning, experimentation, and creative fabrication.

CCS Concepts

• **Human-centered computing → Human computer interaction (HCI)**; *Interaction design.*

Keywords

Self-shaping textiles, bistability, tessellation, pre-stretch fabric, additive manufacturing, tangible interfaces, programmable morphology

ACM Reference Format:
Hye Jun Youn, Jun Kyu Choe, SooYeon Ahn, Marcello Tania, Serena Xin Wei Sara, and Hiroshi Ishii. 2026. PixBric: Precision Morphological Control of Pre-Stretched Fabrics Through Tessellated Primitive Geometries. In *Twentieth International Conference on Tangible, Embedded, and Embodied Interaction (TEI '26), March 08–11, 2026, Chicago, IL, USA*. ACM, New York, NY, USA, 15 pages. https://doi.org/10.1145/3731459.3773316

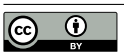

TEI '26, Chicago, IL, USA

ACM ISBN 979-8-4007-1868-7/26/03
https://doi.org/10.1145/3731459.3773316

1 Introduction

Programmable materials capable of controlled shape transformation have emerged as a promising strategy for developing adaptive systems across a range of domains, including soft robotics[11, 23, 35] architectural surfaces[24, 31], and tangible user interfaces [13, 15]. Common mechanisms for achieving shape change—such as pneumatics[5, 14, 46], shape memory alloys [2, 22], and electroactive [30] polymers—often rely on complex fabrication processes and embedded control systems, limiting accessibility and scalability [20, 22].

As a more accessible alternative, recent techniques have explored passive morphing through 3D printing onto biaxially prestretched fabrics [1, 34, 37]. These approaches encode deformation through geometric programming and strain release, enabling self-transforming structures without external actuation [10, 12, 33]. However, most existing implementations rely on heuristics and ad-hoc patterning, offering limited control over morphing behaviors or predictive design [37, 38].

In this paper, we present *PixBric*, a programmable design and fabrication framework that enables precise morphological control of self-shaping textiles through tessellated pixel geometries (Figure 1). By integrating parametric modeling, finite element simulation, and material experimentation, PixBric establishes a structured, reproducible pipeline for programming localized curvature, undulation, bistability, and multistability into stretchable fabrics. The framework supports predictive design by connecting Grasshopper-based Python modeling with an accessible Human UI interface, which is also available via the cloud, and integrating it with finite element analysis in ABAQUS. This workflow enables researchers to anticipate deformation with relative accuracy and fine-tune morphological parameters prior to fabrication. Through empirical evaluation of over thirty configurations and a series of shape-changing prototypes, including morphable typography, wearable artifacts, and reconfigurable surface objects, PixBric contributes a simulation-integrated design framework for HCI and material scientists investigating adaptive interfaces.

PixBric reflects the TEI 2026 theme of *Tide + Tied* by bridging digital simulation (*tide*) with the mechanical constraints of elastic substrates (*tied*). It operates at the intersection of engineering,

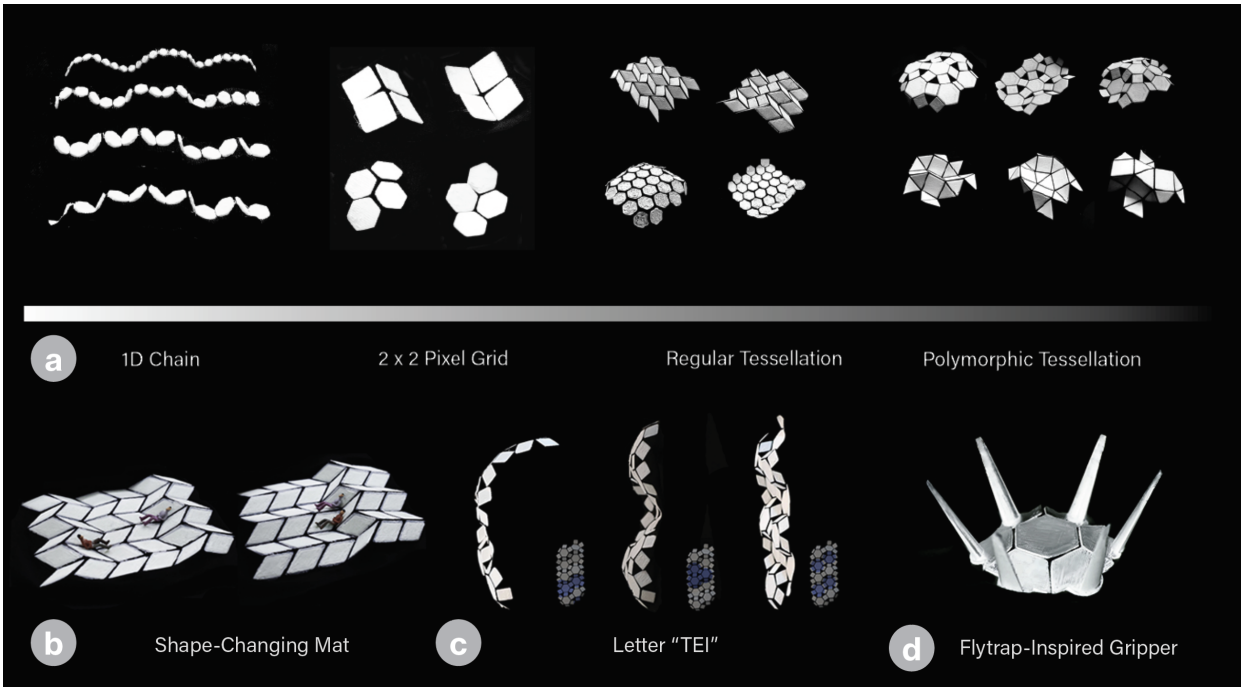

Figure 1: (a)Structural Overview of PixBric from Millimeter to Centimeter Scales. (1) A 1D chain composed of 1–3mm pixels, (2) 2×2 grids of primitive geometries (circle, triangle, rectangle, hexagon) demonstrating bistable behavior, and (3) tessellations exhibiting multiple stable states. Applications (b) Shape-Changing Mat (c) Letter "TEI" (d)Flytrap-Inspired Gripper. All samples were fabricated using a desktop FDM 3D printer.

material science, and design, enabling interactions that are computationally guided yet materially grounded. For TEI researchers, PixBric serves as a tangible design framework linking geometric programming and embodied interaction. For practitioners in computational design, the provided simulation–fabrication pipeline enables accessible experimentation without requiring mechanical expertise. By encoding behavior directly into structure, PixBric demonstrates how geometric intelligence can translate between code and craft—advancing tangible interfaces that are both expressive and functional.

Contributions

Our main contributions are as follows:

- A simulation-integrated design framework maps pixel-based geometric parameters—such as spacing, thickness, and shape—to mechanical behaviors including bending, curvature, and undulation. This enables users to predict and control how 3D-printed fabrics deform, ranging from small local folds to large coordinated transformations. The framework also supports precise tuning of bistability to define stable, semi-stable, or flexible regions within a textile structure.
- A CAD-integrated tool combines parametric modeling in Grasshopper (Rhino) with an accessible Human UI interface and finite element analysis in ABAQUS, enabling designers, engineers, and HCI researchers to visualize and simulate deformation behavior prior to fabrication.
- A metal-frame–based stabilization system for fabric fixation during 3D printing on pre-stretched textiles, with a comparative analysis of magnetic, tape, and clip methods in terms of tolerances, biaxial stretching, repeatability, and reusability.
- An experimental evaluation of over 30 design configurations, measuring snap-through energy, bending angles, and radii of curvature across pixel shapes and scaling ratios—leading to empirically grounded design rules for morphing behavior.
- A set of interactive prototypes, including morphable typography, wearable accessories, and reconfigurable surface objects (e.g., folding mats, bistable brushes), showcasing the system's versatility for tangible computing and adaptive design scenarios.

2 Related Work

2.1 Self-Morphing Pre-Stretched Fabrics

Recent work has shown that 3D printing onto biaxially pre-stretched elastic fabrics enables self-morphing behavior through differential strain release, a phenomenon often referred to as metric frustration [9, 21]. When a stiff material such as PLA or TPU is deposited onto stretched fabric and the substrate is subsequently released, the printed regions resist contraction while the surrounding fabric recoils—producing internal stress gradients that induce predictable out-of-plane deformation.

This contraction-induced morphing mechanism has parallels in bilayer systems and soft actuators, where mismatched strain across

layers generates bending, buckling, or snapping [7, 18, 48]. In tessellated structures like hexagonal or rectangular lattices, anisotropic contraction allows for localized and directional morphing—e.g., vertical links may contract more than horizontal ones, pulling vertices inward to produce curvature [4, 29, 36].

Subsequent studies have adapted this approach to create programmable actuators and shape-shifting forms. Broadly, two passive morphing paradigms have emerged: (1) stimuli-responsive activation, in which materials such as hydrogels or SMAs contract in response to heat or humidity [19, 42, 45, 46]; and (2) stored-strain release, where deformation is encoded during fabrication and triggered upon release—without the need for external stimuli or embedded electronics[27, 32, 39, 43].

A majority of prior work has relied on heuristically selected or visually driven patterns, often composed of arcs, wavy lines, or parametric swirls (Table 1). For example, Fabric Fit [37] employs circular and linear patterns to induce localized deformation and button-like structures; however, the design process remains largely intuitive, offering limited predictive control and requiring iterative physical prototyping to anticipate deformation outcomes.

In contrast, Printed Undulations [10] introduced a more systematic and rational approach by focusing on line-based morphing printed on pre-stretched fabrics. The study evaluated curvature formation as a function of parameters such as temperature, print speed, thickness, and width, supported by simulation. Nevertheless, its investigation was confined primarily to continuous undulation, without extending to other morphing behaviors such as bending, snapping, or bistability.

Among the few works that explore a broader range of geometric behaviors, Embroigami [16] introduced rotated rectangular motifs and mountain–valley fiber patterns, using embroidery (rather than 3D printing) on pre-stretched fabrics to achieve bistable toggling. While these designs demonstrate diverse morphing potentials, they provide limited insight into how primitive parameters—such as spacing, thickness, or material composition—influence the resulting shapes. Moreover, no simulation pipeline or specification of stretching direction is included to support predictive control or design generalization.

While prior works have explored self-morphing textiles, PixBric advances the field by introducing a predictive design workflow that links geometry with material behavior through simulation. Building on this foundation, PixBric uses a tessellation-based framework to create programmable morphing fabrics. By adjusting the distance between pixels and using simple geometric shapes—such as hexagons, rectangles, and triangles—the system can control how the fabric bends and transforms, from small local movements to large coordinated shape changes. The framework also allows designers to encourage or suppress bistability in certain areas, enabling both stable and flexible regions within the same fabric. Altogether, PixBric provides an accessible and adaptable approach for designing self-shaping textiles with customizable mechanical and expressive qualities.

2.2 Reconfigurability in HCI

Reconfigurable physical interfaces enable systems to dynamically adapt their shape, structure, or function in response to user input, environmental stimuli, or task-specific requirements [6, 15, 35]. Unlike many traditional shape-morphing systems that deform irreversibly [9, 25, 47], reconfigurable systems support transitions between multiple stable configurations and enable reversible transformations [27, 28].

A range of actuated systems have demonstrated the potential of reconfigurability in interface design. For example, LineFORM [26]showcased how an actuated rod could morph into various physical configurations—such as a stylus, ruler, or data display—supporting multimodal interactions. Similarly, Transform [8] presented a motor-driven tabletop surface capable of transforming into dynamic landscapes or interactive widgets. These systems exemplify the advantages of reconfigurable interfaces, but rely heavily on embedded actuators, complex control logic, and continuous energy input to maintain their form and function.

Alternative approaches have explored stimuli-responsive materials as a strategy for achieving shape transformation. For example, Yao et al. [CHI, UIST] [40, 41, 44] have demonstrated a range of morphing interfaces utilizing pneumatic actuation, and humidity-thermal sensitive films. These systems enable soft, continuous, and reversible transitions between configurations without the need for rigid mechanical components. While such material-driven methods expand the possibilities of programmable matter, they often necessitate specialized fabrication workflows, precise material calibration, and embedded actuation or control infrastructure—limiting their accessibility and scalability for broader application contexts.

PixBric extends the concept of reconfigurability in HCI by introducing an accessible, precise, and passive material-based framework for shape transformation. PixBric encodes morphing behaviors directly in geometry—through tessellated pixel arrangements (e.g., hexagons, rectangles, triangles) 3D-printed onto biaxially pre-stretched fabric—enabling programmable curvature, localized deformation, and multistability.

3 Precision Morphing Through Tessellated Geometries

3.1 Overview

We present **PixBric**, a systematic end-to-end design framework (Figure 2) for the design and fabrication of programmable, shape-morphing textiles using pixel-based tessellated geometries 3D-printed onto biaxially pre-stretched elastic fabrics. The pipeline integrates four key stages—**Tessellation Design**, **Simulation**, **Fabrication**, and **Morphing Output**—to enable precise control over mechanical deformation behavior.

- **Tessellation Design:** Parametric grids (e.g., hexagonal, rectangular) are generated in computational tool human ui, with optional modulation by image brightness to vary local geometry size and spacing.
- **Simulation:** Morphing behavior is predicted using finite element analysis (ABAQUS), modeling fabric and PLA components with distinct material properties.
- **Fabrication:** Designs are printed directly onto pre-stretched fabric using a custom designedmagnetic framing system to ensure uniform biaxial tension. Upon release, the fabric transforms into preconfigured 3D shapes.

Table 1: Comparative chart evaluating prior work based on device type, morphing method, pattern design strategy, stretching direction, bistability, and simulation integration. Color encodes performance: bright green = strong, light green = moderate, yellow = limited, pink = lacking.

Precedent	Tool	Morphing Method	Pattern Design Decision	Stretching Direction	Bistability	Simulation
FabricFit [37]	FDM	High temperature	**Arbitrary:** line/circle placement without defined sizing logic.	Not specified (likely biaxial)	✗	✗
Flexmock [38]	Attached patterns	Pre-stretched Fabric	**Arbitrary:** auxetic motifs without mathematical reasoning or programmed variation.	Not specified	✗	✗
Embedded Textile [34]	FDM	Glue, string	**Arbitrary:** primitives applied without structured rules.	Uniaxial	✗	✗
Buckled Geometry [3]	FDM	Pre-stretched Fabric	**Arbitrary:** limited geometry exploration; unclear design logic.	Uniaxial	△ Not specified	✓ (FEA/ABAQUS)
Undulation [10]	FDM	Pre-stretched Fabric	**Reasonable:** varies line thickness/print speed to control undulation.	Biaxial	✗	✓ (FEM)
Printing-on-Fabric [17]	FDM	Pre-stretched Fabric	**Reasonable:** adjusts scale/spacing of star pattern; evaluates one design.	Biaxial	△ Not specified	✓ (custom)
Active Membranes [1]	FDM	Pre-stretched Fabric	**Reasonable:** curvilinear patterns with clear parameter control (limited diversity).	Biaxial/Uniaxial	✗	✓ (FEM + models)
Embroigami [16]	Embroidery	Pre-stretched Fabric	**Reasonable:** primitive geometry; lacks systematic spacing rules or simulation.	Not specified (likely biaxial)	✓	✗
PixBric (this work)	FDM	Pre-stretched Fabric	**Reasonable:** systematic primitives with parametric spacing/scale rules; simulation-backed design.	**Biaxial**	✓	**Yes ✓ (ABAQUS)**

- **Morphing Output:** The final structures exhibit localized or gloval deformation, bistability and more , enabling programmable shape change suitable for interactive textiles and adaptive interfaces.

3.2 Human-UI Parametric Design Tool

To enable customized tessellated designs for desired morphing behaviors, we developed a computational design platform using Rhinoceros 3D and its visual programming plug-in, Grasshopper (Figure 3). In addition, the Grasshopper Human UI interface and our web-based parametric design repository provide interactive sliders for adjusting pixel geometry, spacing, and pre-stretch ratios, supporting accessible and intuitive experimentation.

3.2.1 Tessellation of Primitive Geometry. The workflow begins by defining a base grid structure using Grasshopper components. This grid is then populated with geometric primitives that serve as the fundamental "pixels" of the textile. Parameter sliders are implemented through the Human UI interface to adjust variables such as:

- **Pixel geometry:** selection between triangle, square, and hexagon modules;
- **Pixel scale:** global and local scaling factors controlling deformation intensity;
- **Inter-pixel spacing:** controlling the degree of mechanical coupling and flexibility between adjacent pixels;
- **Thickness:** extrusion height of each pixel pattern, determining the stiffness and bending response of the printed structure. The extrusion is defined parametrically in Grasshopper using the *Extrude* component, allowing uniform or gradient-based variation across the surface.

3.2.2 2D Image to Textile Conversion. To support data-driven tessellation and enable the translation of visual imagery into morphing textile structures, we developed a custom Python script embedded within Grasshopper. The script processes 2D images—such as photographs, drawings, or grayscale heightmaps—and converts their pixel information into geometric parameters for 3D printing, automatically scaling the output to fit within the physical dimensions of the 3D printer bed. The Grasshopper plug-in, Human-UI interface, and example project files are released as supplementary materials and available via our GitHub repository.

The workflow begins by importing an image through Grasshopper's *Import Bitmap* component or the integrated Human UI file selector. The script then extracts per-pixel brightness values from the image. These luminance values are normalized to a range of [0–1] and stored as a data matrix that corresponds spatially to the target tessellation grid.

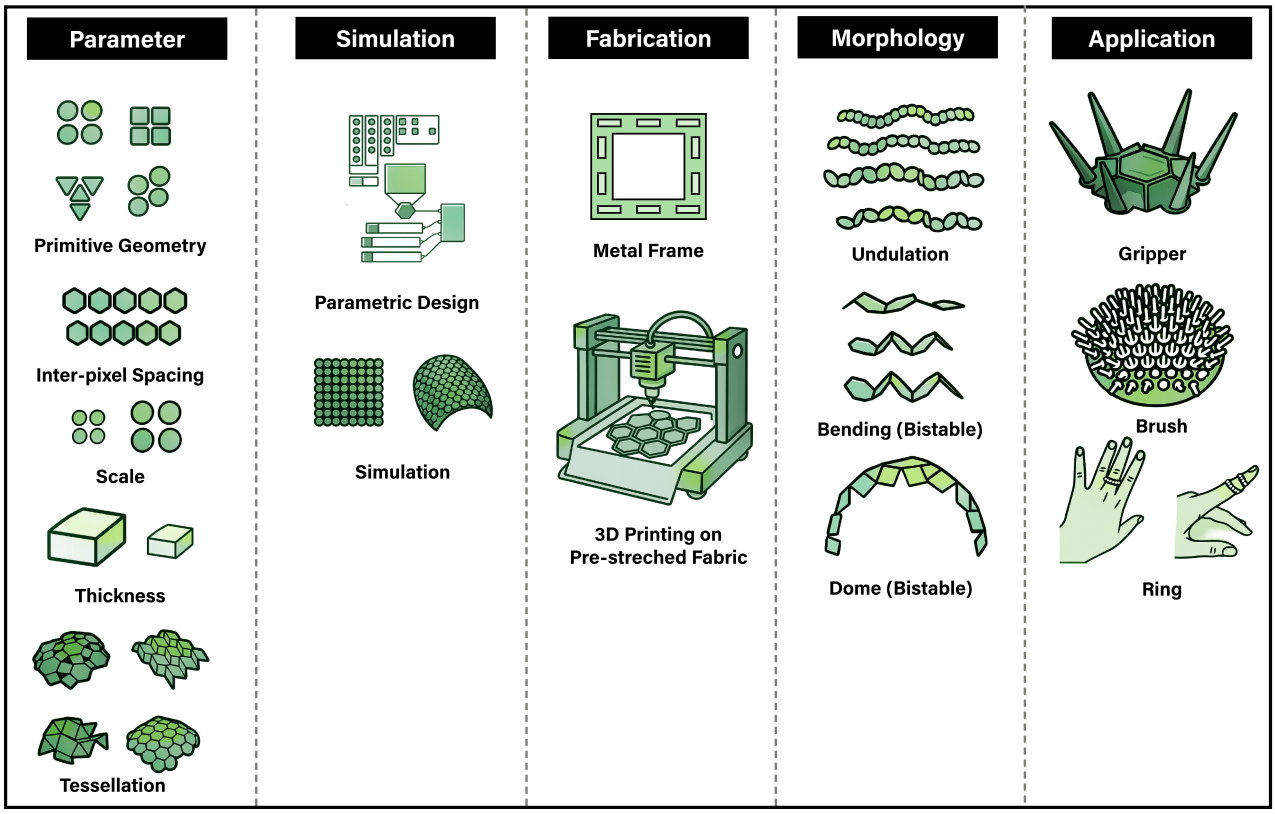

Figure 2: Overview of the PixBric framework. From fabrication to application, showing the relationship between fabrication setup, simulation, design parameters, resulting morphologies, and tangible applications such as grippers, brushes, and wearable rings.

Each value is mapped to a geometric modifier controlling parameters such as:

- **Max and min Pixel size:** brightness values determine the diameter or side length of each hexagonal unit; darker regions produce larger hexagons, while lighter regions generate smaller ones;
- **Max and min inter-pixel spacing:** inter-pixel distance adapts based on local brightness gradients to control flexibility and coupling between units.

The hexagonal lattice was chosen for its space-filling efficiency, isotropic mechanical behavior, and aesthetic continuity when representing complex imagery. Users can also switch to alternative primitives—rectangular or triangular units—via dropdown controls within the Human UI interface. The mapping function supports both direct and inverse scaling modes, allowing users to determine whether darker regions should expand or contract geometrically.

Once the brightness-to-geometry mapping is complete, the resulting tessellated surface can be visualized in real time in the CAD environment and exported directly as an STL file for 3D printing. The same model can also be transferred to the simulation pipeline (ABAQUS) for deformation analysis, allowing users to preview morphing behavior before fabrication.

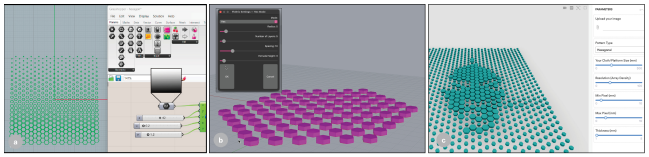

Figure 3: Parametric design tools. (a) Conversion from 2D patterns to textile geometries in Rhino Grasshopper, mapping image brightness to pixel geometry, scale, and spacing for localized morphing control. (b) Human UI interface within Rhino for real-time parameter adjustment, including thickness, shape, and array configuration. (c) Cloud-based Human UI interface via ShapeDiver for accessible, browser-based interaction.

3.3 Simulation

To predict self-shaping behavior and reduce reliance on time- and resource-intensive physical prototyping, we conducted finite element simulations using ABAQUS (Dassault Systèmes), a widely accessible platform for HCI researchers. This simulation pipeline enables rapid iteration and early validation of morphing outcomes,

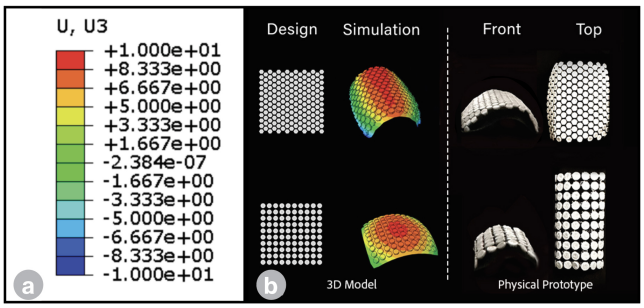

Figure 4: (a) Displacement along the Z-axis (unit: mm)(b) Simulation of hexagonal and circular pixel tessellations..

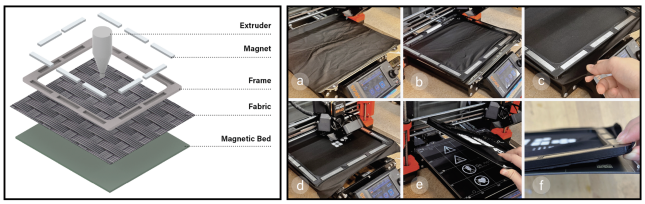

Figure 5: (Left)Installation of the magnetic frame on a 3D printer (Prusa MK4S. (Right) (a) Place the pre-cut fabric, (b) attach the magnetic frame, (c) stretch the fabric biaxially, (d) start 3D printing, (e) carefully remove the print from the printer, and (f) separate the fabric from the bed.

allowing designers to estimate deformation behavior prior to fabrication (Figure 4).

3.3.1 Simulation Setup. To simulate the morphing behavior of the PixBric system, geometries were first created in parametric tool and exported to ABAQUS for finite element analysis. The system was modeled as a composite structure consisting of a deformable textile substrate and embedded PLA pixel units.

The textile layer was represented as a 3D deformable shell using S4R (reduced integration, quadrilateral) elements, with material behavior defined by the Holzapfel-Gasser-Ogden (HGO) hyperelastic model to capture the anisotropic characteristics typical of woven or knitted stretch fabrics. The material parameters were set as $C_{10} = 0.01$ MPa, $k_1 = 0.4$ MPa, $k_2 = 0.03$ MPa, and $lpha = 0.3$.

To simulate prestrain behavior, we introduced a 50% biaxial in-plane contraction through orthotropic thermal expansion coefficients, emulating the effects of fabric pre-stretch and release during fabrication.

The PLA pixel units were modeled as 3D deformable solids using C3D8R brick elements, with linear elastic properties assigned to reflect typical PLA behavior: a density of 1,250 kg/m^3, Young's modulus of 2,890 MPa, and a Poisson's ratio of 0.35.

3.3.2 Comparison to Physical Behavior. To validate simulation fidelity, we conducted a comparative study between finite element analysis (FEA) predictions and physical deformations observed in fabricated samples. Specifically, we tested 10×10 mm circular and hexagonal pixel geometries, spaced 1 mm apart and printed with 1.0 mm thick PLA (polylactic acid) filament onto fabric pre-stretched biaxially to 150%.

Upon release, circular pixels exhibited smooth, dome-like curvatures, while hexagonal pixels demonstrated sharp, directional bending along their long axis. These distinct deformation modes were successfully replicated in simulation, with the predicted morphologies closely matching those captured in post-release photographs.

The simulated radius of curvature and principal bending axes aligned with the observed physical results, confirming that the model accurately reflects the mechanics of prestrain-driven shape transformation. This lays the groundwork for predictive design of programmable morphing textiles based on computational modeling.

3.4 Fabrication: 3D Printing on Pre-Stretched Fabric Using a Magnetic Frame

We developed a rapid and accessible method for 3D printing onto biaxially pre-stretched fabric using an off-the-shelf magnetic framing system (Figure 5). The magnetic frame is designed to be compatible with 3D printers that use magnetic beds (e.g., Prusa MK4S). Neodymium magnets (≥5 mm thick), embedded along the frame edges and 3D-printed into the frame structure, securely hold the fabric during printing, with three magnets on each edge. A frame height of 6 mm ensures clearance from the extruder. The fabric is biaxially pre-stretched to 150% and mounted within the frame prior to printing. For all experiments, we used a two-way stretch tricot fabric (T6008), composed of 80% spandex and 20% cotton. Models were printed using a 0.4 mm nozzle with standard PLA settings: 235 °C extrusion temperature and 250 mm/s print speed.

The fabrication process begins by pausing the 3D printer before the first layer using a custom G-code pause inserted in PrusaSlicer. During this pause, the fabric is manually stretched and secured onto the print bed using a custom magnetic frame. To ensure accuracy and repeatability, the frame was equipped with grid markings for precise alignment, allowing each fabric sheet to be stretched to a target ratio of 130%. Once properly aligned, printing resumes, allowing the molten filament to strongly adhere to the tensioned textile surface. After printing is complete, the fabric is removed, the perimeter is trimmed, and upon release of tension, the printed regions buckle into their pre-designed three-dimensional forms.

3.5 Comparison of Fabric Stabilization Methods

We compared three fixation approaches for maintaining tension during 3D printing on pre-stretched textiles: tape-based, clip-based, and magnetic-frame stabilization (Table 2). The magnetic frame demonstrated clear advantages across setup efficiency, uniformity of tension, and repeatability of morphing results. Unlike tape or clips, which rely on localized points of adhesion or clamping, the magnetic frame distributes tension evenly along all edges, ensuring consistent biaxial pre-stretching. This uniformity is essential for achieving reproducible morphing behavior, as small inconsistencies in tension can significantly alter curvature and bistability.

In practical terms, the magnetic frame enabled rapid mounting and removal of fabric samples, reducing setup time. Tape fixation often failed under secondary-axis stretching, tearing or detaching from the bed, while clips introduced uneven tension and local

buckling near attachment points. By contrast, the magnetic frame maintained stable adhesion and even stress distribution across both the X and Y axes throughout the printing process.

Uniform biaxial stretching proved critical for consistent shape transformation. A controlled 10% imbalance between the two axes produced a measurable bending bias toward the lower-tension direction, accompanied by smaller deformation angles, confirming the sensitivity of morphing behavior to anisotropic stress.

Repeatability testing across ten fabrication cycles confirmed the stability of the magnetic frame, showing an average bending deviation of only ±3.2%—significantly lower than the irregular deformation and variability observed with tape and clip methods. These results demonstrate that the magnetic frame provides a simple and reliable means of achieving consistent biaxial pre-stretching for textile-based morphing fabrication.

4 Evaluation and Design Principles

4.1 Material Compatibility and Fabric Selection

We evaluated six fabric types—cotton, nylon, spandex, mesh, and various multi-material blends—based on key mechanical and surface properties, including stretchability, elasticity, porosity, and surface friction, to determine their compatibility with self-shaping morphologies. These parameters directly affect a fabric's ability to support bistable deformation, facilitate reliable adhesion during 3D printing, and maintain structural integrity after actuation.

Highly porous fabrics, such as polypropylene mesh, exhibited excessive filament seepage during printing, requiring a two-step fabrication process. A base PLA layer was first printed directly onto the print bed before placing the fabric, improving adhesion and preventing leakage. This approach ensured cleaner interfaces but introduced additional complexity and material usage. In contrast, low-porosity fabrics—such as dense cotton and spandex composites—enabled direct deposition of PLA without the need for a base layer, as the filament adhered securely to the textile surface even in the absence of encapsulation. In these cases, the first layer could be omitted without degrading print fidelity or morphing performance.

Spandex-based fabrics stood out for their superior stretch and elastic recovery, which are critical for supporting reversible, snap-through behaviors in bistable structures. However, their low surface friction occasionally led to nozzle drag and minor distortion during deposition, particularly on unsupported areas of the print bed.

Based on these findings, we selected a two-way stretch tricot fabric composed of 80% spandex and 20% cotton as the default substrate for all subsequent experiments. This material offered a strong balance of mechanical compliance, moderate porosity, and consistent print adhesion, minimizing fabrication artifacts while enabling reliable, repeatable shape transformations across a wide range of morphing prototypes.

4.2 Morphing Behavior: Parameters and Mechanics

This section systematically investigates how geometric parameters—including unit shape, scale, inter-pixel spacing, and thickness—govern the mechanical response of the structure. Through controlled variation of these factors, we identify configurations that induce localized versus global deformation modes, support bistable transitions, maintain flat states, or produce undulating surface morphologies.

4.2.1 Pixel Geometry and Shape Effects. We evaluated four primitive geometries—circles, triangles, rectangles, and hexagons—arranged in 2×2 and 3×3 tessellated grids (10 mm width, 1 mm thickness, 1 mm spacing) to investigate how unit shape influences morphing behavior (Figure 6). The resulting deformation patterns are governed by vertex connectivity (i.e., the number of edges converging at each node) and the topological arrangement of adjacent tiles, which together determine the structure's degrees of freedom, mechanical coupling, and global deformation modes (Table 3).

Triangular pixels, characterized by six edges converging at each vertex and internal angles of 60°, form highly constrained networks that restrict local movement. As tessellation density increases, the structure behaves as a collective sheet, producing broad, synchronized deformations but fewer distinct bistable regions. These over-constrained configurations favor large-scale curvature rather than localized snapping.

Rectangular pixels, composed of four edges per vertex with 90° angles, strike a balance between rigidity and flexibility. Their orthogonal topology enables moderate inter-unit coupling while still

Table 2: Comparison of magnetic, tape, and clip methods for fabric stabilization during 3D printing on pre-stretched textiles, including tolerances and repeatability metrics.

Method	Fabric Stabilization	Setup Time	Risk Level	Reusability	Evenness	Tolerances / Repeatability
Tape	**Unstable:** Peels under high tension.	**3–5 min:** Requires careful taping.	**Safe.**	**Reusable only 2–3 times.**	**Uneven tension.**	**±10-30% error:** Large variability between prints; cannot be biaxially stretched.
Clips	**Somewhat stable:** Dependent on placement.	**10–15 min.**	**Unsafe:** May detach unexpectedly.	**Reusable up to ~10 times.**	**Uneven tension.**	**±10-20% error:** Moderate repeatability with slight variation.
Magnetic Frame (our method)	**Stable:** Maintains uniform tension.	**1–2 min:** Fast setup.	**Somewhat safe:** Handle magnets carefully.	**Reusable 50+ times.**	**Even:** Consistent in X/Y directions.	**±3–5% error:** High repeatability across 10 tests; minimal variation in bending angle.

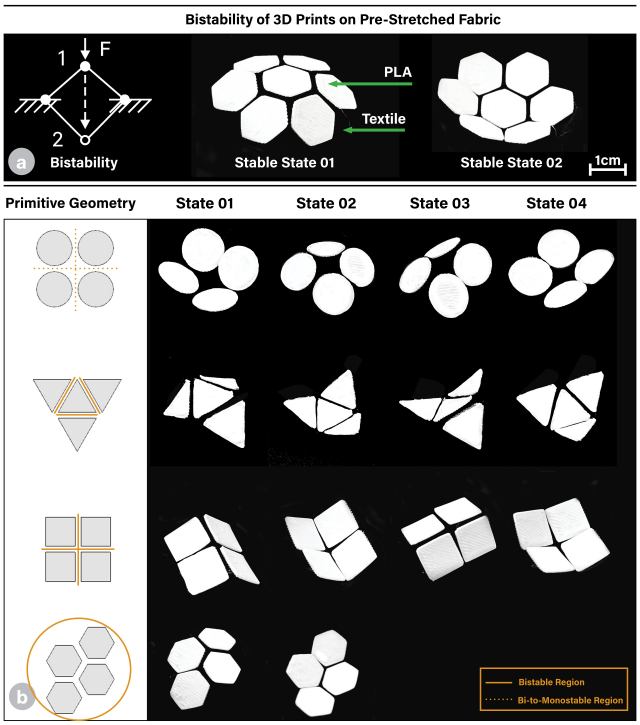

Figure 6: (a) Design Atlas illustrating bistability principles through hexagonal global deformation. (b) Morphological stable states across primitive geometries—circles, triangles, rectangles, and hexagons. Orange solid lines denote bistable regions, while orange dashed lines indicate monostable regions.

allowing localized shear and bending, producing multiple bistable configurations that increase with tessellation density—from four stable states in smaller grids to over ten in larger arrays.

Hexagonal pixels, defined by three edges per vertex and 120° angles, act as compliant hinge-like joints that efficiently propagate deformation across the lattice. Their isotropic packing and geometric uniformity facilitate smooth transitions between monostable and bistable states. Notably, the number of bistable states remained constant (two) across different tessellation densities, indicating stable, predictable deformation behavior.

Circular pixels, in contrast, lose structural bistability even when the inter-pixel spacing is 1 mm, behaving as monostable membranes with limited shape retention due to uneven stress distribution across the structure. Collectively, these topological differences define intrinsic mechanical constraints that determine whether deformation occurs locally or propagates globally. (Table 4).

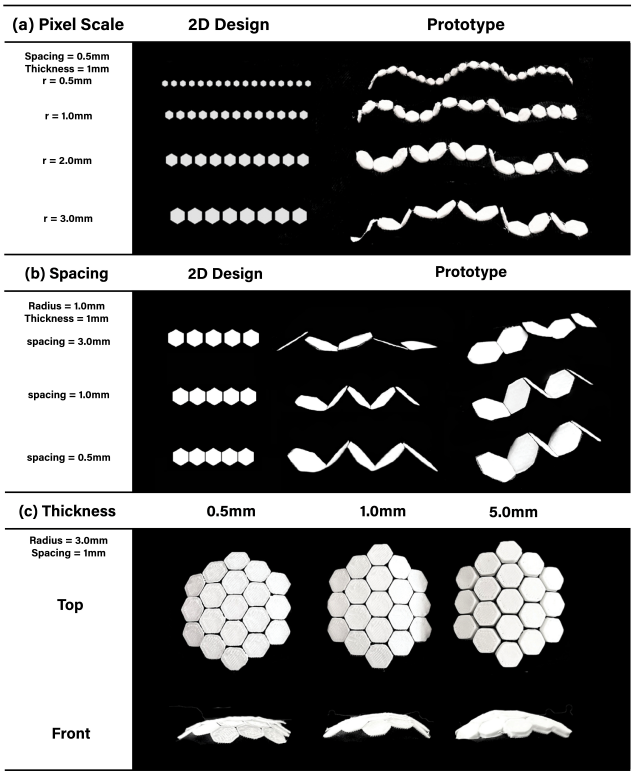

Figure 7: Hexagonal pixel arrays with varying inter-pixel spacing (0.5–3mm). Arrays with 0.5–2mm spacing maintain bistable configurations, while 3mm spacing results in monostable behavior due to insufficient mechanical coupling.

4.2.2 Pixel Scale. The scale of each hexagonal pixel—ranging from 1 mm to 20 mm in width with a constant 1 mm inter-pixel spacing—strongly influenced curvature formation and overall morphing dynamics while maintaining snap-through bistability. Smaller pixels (0.5–2 mm) produced finely distributed deformations, enabling continuous undulating surfaces that smoothly transitioned between stable states. These configurations exhibited high coupling with the fabric substrate, allowing stored elastic energy to propagate evenly across the structure.

Table 3: Observed number of stable states across different primitive geometries and tessellation densities.

Primitive Geometry	2×3 Tessellation	3×3 Tessellation	4×4 Tessellation
Circle	1 (loses bistability; becomes monostable)	1	1
Triangle	8	8	N/A
Rectangle	4	10	14
Hexagon	2	2	2

Table 4: Design summary: relationship between pixel geometry, fabrication parameters, and morphing behavior usnig 3d printer.

Geometry	Thickness (mm)	Inter-pixel spacing (mm)	Radius	Morphing Behavior
Circle (dots)	0.5–2.5	0.5–1.0	0.5–2	**Mono-stable:** Exhibits gentle undulation and local curvature when $r < 1$ mm and spacing < 0.5 mm. Higher spacing (> 1 mm) loses bistability. Suitable for wavy surface textures.
Rectangle	0.5–2.5	0.5–3.0	0.5–5	**Bi-stable:** Four-edge vertices allow localized shear deformation, producing hinge like snappable, angled bending.
Triangle	0.5–1.0	0.5–3.0	0.5–5	**Bi-stable:** angles of 60°, form overconstrained networks that limit local degrees of freedom and typically induce large-area, collective deformation
Hexagon (honeycomb)	0.5–2.5	0.5–3.0	0.5–5	**Bi-stable:** high packing efficiency promote continuous global deformation
Tessellation	mixed	0.5–3.0	mixed	**Multi-stable:** Multi-stable: Mixed primitive geometries enable curvature modulation, allowing selective control between large-area collective and localized deformation

Rules of thumb: Smaller spacing (0.5–1.0 mm) (↓) increases the energy barrier and enhances bistability.
Vertex connectivity (edges per node) dictates deformation scale: triangles—collective; hexagons—global; rectangles—localized.

In contrast, larger pixels (≥3 mm) behaved as more isolated, button-like elements that localized deformation within small clusters (typically 2–3 units). The increased rigidity and reduced areal density weakened inter-pixel coupling, leading to discontinuous surface transformations and diminished global curvature.

4.2.3 Inter-Pixel Spacing. This experiment examines how inter-pixel spacing influences the self-shaping stability of pre-stretched textile structures (Figure 7). Hexagonal pixels—selected for their uniform geometry and isotropic strain distribution—were arranged with spacings from 0.5 mm to 3 mm. Optimal morphing occurred within the 0.5–2 mm range, where stored elastic energy was efficiently released upon relaxation, producing strong, repeatable dome-like deformations with clear bistable snap-through transitions driven by uniform strain distribution and effective pixel coupling.

Beyond 2.5 mm spacing, mechanical coupling weakened, limiting in-plane force transmission and reducing out-of-plane deformation. These structures exhibited diminished bistability and flatter, monostable morphologies, underscoring inter-pixel spacing as a critical parameter governing the mechanical behavior and overall performance of morphing fabrics.

4.2.4 Pixel Thickness. In addition to geometry, pixel thickness plays a critical role in determining the magnitude and stability of morphing behavior. An optimal thickness range of 0.5–2,mm was identified. Within this range, the printed structures exhibited strong elastic recovery and reliable bistable transitions, as the thickness provided sufficient stiffness to maintain form while remaining flexible enough to respond to fabric contraction.

When thickness exceeded 3,mm, however, the added mass and rigidity of the printed regions began to suppress deformation, particularly on fabrics with lower elasticity. These thicker structures resisted bending and often failed to return to their original state, resulting in flattened or partially deformed morphologies. Conversely, excessively thin prints (<0.5,mm) lacked the structural integrity to retain curvature and were prone to delamination during post-release relaxation.

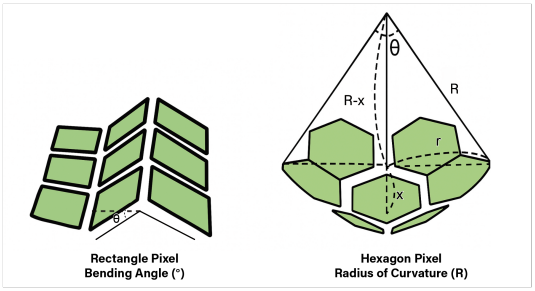

Figure 8: (a) Bending Angle and Curvature Measurement through Experimental and Simulation Analysis

4.3 Experimental and Simulation Analysis

To evaluate morphing performance across different pixel parameters, we conducted a comprehensive geometric analysis focusing on two key deformation metrics: the radius of curvature for hexagonal configurations and the bending angle for rectangular patterns (Figure 8). To quantitatively estimate the energy barrier associated with these bistable transitions, we conducted snap-through experiments using calibrated weights.

This analysis was performed using two parametric scaling strategies designed to isolate the effects of geometric proportion and spatial coupling. In the first approach—*proportional scaling* (R1)—both pixel width and inter-pixel spacing were increased simultaneously while maintaining a constant width-to-spacing ratio. In the second approach—*fixed spacing* (R2)—the pixel width and height were increased incrementally, while the inter-pixel spacing was held constant at 1mm and the thickness at 1mm, to isolate the influence of pixel size on coupling strength and morphing performance. Each parameter combination was tested across 15 repetitions to ensure measurement consistency and statistical robustness.

4.3.1 Bending Angle and Radius of Curvature. For rectangular pixel arrays under proportional scaling (R1), high bending angles ranging from 80° to 94° were achieved at smaller pixel widths between 10–20 mm (Figure 9). As the pixel size increased beyond this range,

the structures gradually flattened due to reduced in-plane tension and increased gravitational loading.

In contrast, the fixed-spacing condition (R2) maintained bending behavior across a wider range of pixel sizes. Although the overall bending angle decreased slightly with increasing pixel width—largely due to added material stiffness and weight—the structures continued to exhibit clear deformation even up to 30 mm pixels. This result demonstrates that maintaining a constant inter-pixel spacing of 1 mm preserves strong mechanical coupling between adjacent pixels, ensuring more uniform strain distribution and sustained curvature despite the increase in scale.

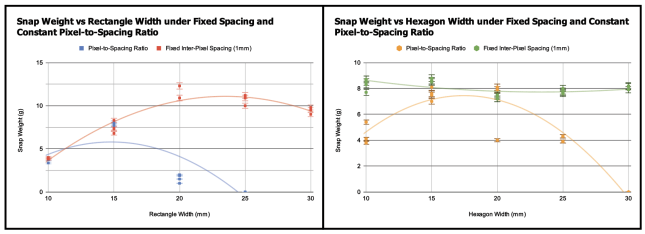

Figure 10: Energy barrier required to trigger snap-through transitions in rectangular (left) and hexagonal (right) pixels under fixed 1 mm spacing and a constant pixel-to-spacing ratio.

For hexagonal configurations, the curvature was quantified using the standard arc approximation formula:

$$R = \frac{x^2 + r^2}{2r} \tag{1}$$

where x is half the chord length (representing the horizontal span of the arc), r is the sagitta height (the vertical distance from the chord to the apex), and R is the resulting radius of curvature. This method allowed for the precise estimation of dome-like deformations and provided a comparative basis for evaluating different pixel dimensions.

Under proportional scaling (R1), as pixel size increased, the structures consistently exhibited smooth, ovule-shaped curvature characterized by a large radius of deformation. In contrast, the fixed-spacing configuration (R2) reveals the overall radius of curvature gradually decreased with increasing pixel dimensions.

4.3.2 Bistability. Bistability for each prototype was evaluated by placing calibrated weights at the center of a 3×3 pixel array while keeping the fabric edges fixed to prevent boundary movement. The displacement at the snap-through point was measured using photographic documentation and manual comparison of deformation frames. This setup provided a consistent method to estimate the minimum energy required to trigger shape change and to compare activation thresholds across different pixel geometries and configurations (Figure 10). We applied this procedure to both rectangular and hexagonal tessellations under two scaling strategies: proportional scaling (R1) and fixed spacing (R2).

For rectangular pixels, proportional scaling (R1) achieved bistable behavior at smaller widths (10–20 mm), but bistability declined sharply beyond 20 mm and disappeared entirely around 25 mm. In contrast, the fixed-spacing condition (R2) maintained bistability even at larger pixel widths up to 30 mm. Although the bending angle decreased slightly due to increased weight, the structures preserved stable snap-through behavior, showing that maintaining

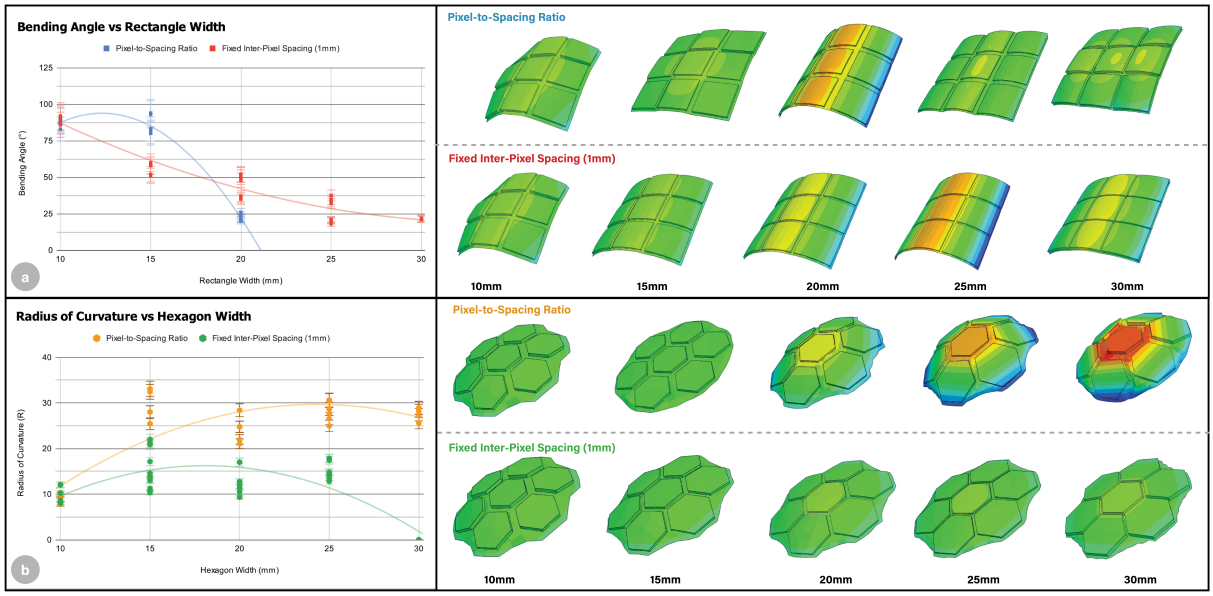

Figure 9: (a) (Left) Experimental measurement of bending angles in rectangular tessellations with varying pixel-to-spacing ratios (fixed spacing = 1 mm, thickness = 1 mm). (Right) Corresponding finite-element simulation results in ABAQUS. (b) (Left) Measured curvature of hexagonal tessellations. (Right) Comparison with ABAQUS simulation results.

Table 5: Summary of application prototypes linking geometry, key parameters, stability, and purpose.

Application	Geometry Type	Key Parameters	Stability	Purpose
Ring	Hexagonal tessellation	Width: 0.5 mm; Spacing: 0.5 mm	Bi-stable	Conforming wearable that adapts to finger curvature through bistable deformation.
Hairbrush	Hexagonal lattice (scale-varying)	Spacing: 0.5–1.5 mm; Thickness: 1 mm	Bi-stable	Foldable, impact-absorbing surface designed for transportation.
Morphing Typography (TEI)	Hybrid (hexagonal + rectangular)	Spacing: 1 mm; Thickness: 1.5 mm	Multi-stable	Expressive morphing typography combining localized and global deformation through polymorphic tessellation.
Adaptive Mat	Diamond / polymorphic lattice	Variable spacing: 0.5–2.0 mm	Multi-stable	Reconfigurable comfort surface that adjusts shape through touch or applied pressure using regular tessellation.
Gripper	Hexagonal lattice	Spacing: 1 mm; Thickness: 1 mm	Bi-stable	Passive gripping structure enabling object capture.

a constant inter-pixel spacing of 1 mm ensures stronger coupling and more reliable bistability at larger scales.

For hexagonal pixels, similar patterns were observed. Under proportional scaling (R1), bistability diminished rapidly when pixel width exceeded 25 mm and was lost entirely near 30 mm, resulting in flat, monostable morphologies. However, under fixed spacing (R2), bistability was consistently maintained across all tested pixel widths, with stable dome-shaped curvature and strong snap-through transitions.

Overall, proportional scaling (R1) often lost bistability and morphing fidelity at larger scales, whereas fixed spacing (R2) preserved bistability and curvature across a wider range of geometries. These results highlight the trade-off between scalability and energy efficiency in morphing textile systems.

5 Applications

This section demonstrates the versatility of the PixBric system through a series of application scenarios that exploit its programmable morphologies and tunable mechanical stability. Each prototype directly builds on the design-space parameters established in previous sections—linking pixel geometry, spacing, and thickness to specific morphing outcomes. The case studies span adaptive mat, wearable accessories, expressive typography, and passive gripping, collectively illustrating how parameter-driven control enables functional and aesthetic applications of programmable textiles. (Table 5)

5.1 1D Array of Pixels for Accessories

We developed finger-conforming accessories using one-dimensional arrays of hexagonal pixels, each with a 0.5mm width and 0.5mm inter-pixel spacing. These linear ring prototype structures exhibit inherent bistability, enabling them to retain undulating geometries in their resting state while conforming adaptively to body contours upon contact. The mechanical flexibility embedded in the geometry allows the ring to deform and recover without losing its structural integrity, accommodating a variety of finger sizes without requiring changes to the base design (Figure 11).

By parametrically modulating pixel spacing and scale along the array, we achieved tunable curvature and directional flexibility

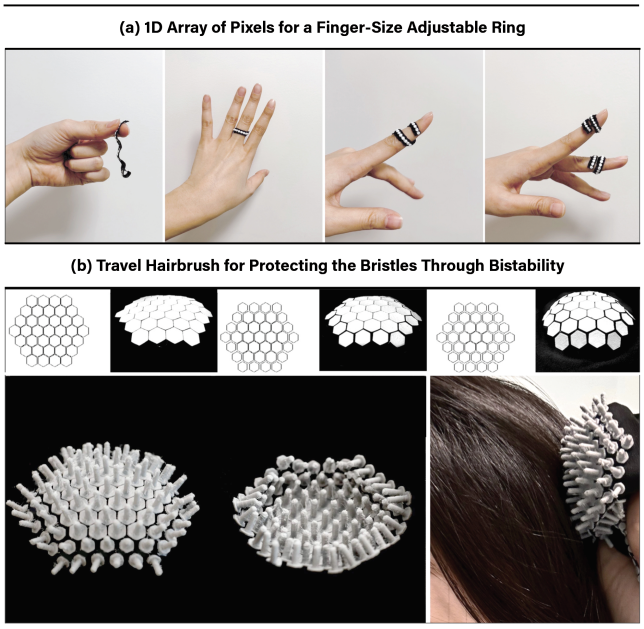

Figure 11: (a) Ring Adaptable to Various Finger Thicknesses Using a 1D Chain with 0.5mm Spacing and 0.5mm Width; (b) Bistable 3D-Printed Hairbrush Formed by Varying Pixel Scale on Pre-Stretched Fabric.

suitable for wearables. This approach eliminates the need for size-specific models or embedded electronics, instead relying on geometric intelligence to create responsive, body-conforming structures. The resulting accessory combines comfort, adaptability, and resilience in a lightweight, passive form. This design strategy highlights the broader potential of programmable morphing geometries for creating adaptable, reconfigurable wearable systems—expanding the design space for passive, form-fitting accessories that require no active actuation or user-specific customization.

5.2 Foldable Hairbrush

This hairbrush prototype employs a tessellated hexagonal lattice with scale-varying pixels, each incorporating a bistable, dome-shaped pin. Unlike conventional hairbrushes that are prone to fracturing under sudden force or during transport, the globally bistable domes in this design enable reversible folding, effectively

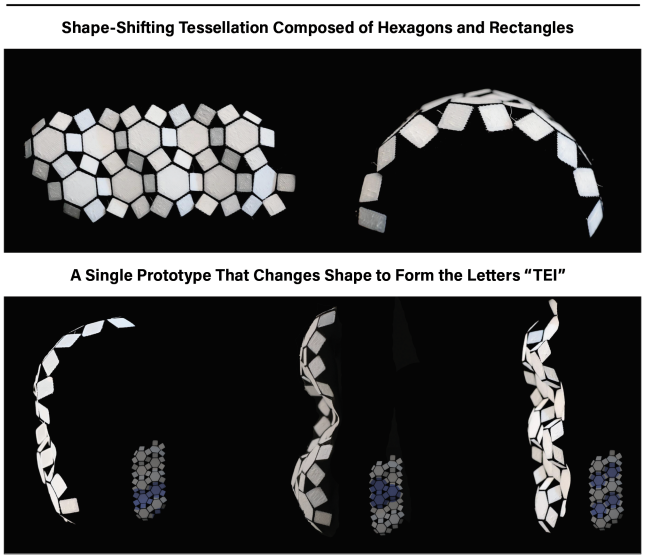

Figure 12: The word "TEI" formed using a combination of hexagonal and rectangular tessellations, each exhibiting multiple stable states.

redistributing impact forces across the structure. This passive mechanical response enhances durability, allowing the brush to absorb greater loads without experiencing structural failure or permanent deformation.

The bistable pins reliably return to their original configuration once the applied force is removed, ensuring long-term resilience and consistent functionality over repeated use. Dome geometries were parametrically generated by modulating inter-pixel spacing within a hexagonal grid, with curvature emerging from programmable geometric differentials that tune snap-through behavior. This setup allows uniform snapping across the brush surface, minimizing stress concentrations and maximizing mechanical compliance.

Beyond durability, the bistable response supports practical improvements in portability: the domes can temporarily collapse to reduce volume, protecting the pins during travel or storage and enabling the brush to fit into compact spaces without specialized cases. The design thus presents a robust, reconfigurable alternative to traditional brushes—demonstrating the broader potential of morphable textile-based materials in creating resilient, adaptable, and user-friendly everyday objects.

5.3 Tessellation for Lettering

We developed a morphable lettering system using a hybrid tessellation of hexagons and rotated rectangles. Leveraging multistability, each pixel can snap between flat and dome-like states, enabling reversible transitions across a variety of letterforms, including the demonstration case of "TEI" (Figure 12).

Each pixel operates independently, with a 1mm inter-pixel spacing between hexagons and rectangles. This arrangement allows hexagonal regions to induce broader, global deformations, while rectangular pixels support localized morphing without disturbing surrounding areas. The programmable bistability enables selective actuation of specific regions. The geometric design ensures a balance between mechanical stability and flexibility, allowing for controlled and repeatable reconfiguration.

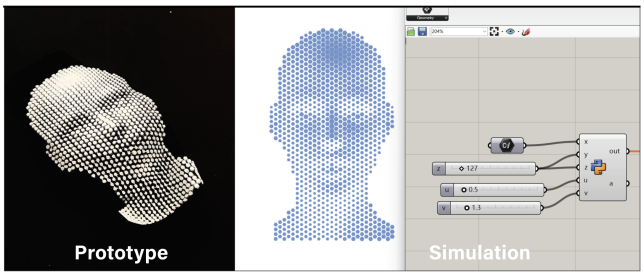

Figure 13: A fabric structure whose curvature is derived from a 2D grayscale image, with pixel size mapped to brightness values to encode shape.

5.4 2D-to-3D Transformation of Complex Structures

Using a custom Grasshopper-based parametric design tool, we convert 2D image data into morphable 3D textile structures through the strategic placement of hexagonal honeycomb pixels (Figure 13). This image-driven framework maps geometric parameters—such as pixel size, spacing, and orientation—to luminance gradients and spatial features extracted from the source image, enabling precise and localized control over mechanical deformation behavior. Luminance values are normalized and translated into pixel scale modulations, where darker regions yield larger, more deformable hexagons, and lighter regions result in smaller, stiffer ones.

By tuning these distribution rules, designers can embed spatially varying curvatures that correspond to visual motifs. The resulting structures exhibit both functional and expressive characteristics—such as dome-like curvature, undulation, or flat resting states—based solely on the pixel geometry and its spatial organization.

5.5 Shape-Changing Mat: Responsive Surface for Adaptive Comfort

We developed a shape-morphing mat based on a diamond tessellation composed of bistable units that can be locally reconfigured through direct physical interaction. Designed for outdoor or dynamic settings, users can selectively deform specific regions into supportive geometries tailored to various postures or activities (Figure 14). Unlike conventional mats with static topologies, this system enables on-demand morphological adaptation: pressing, folding, or sliding targeted areas triggers snap-through transitions, shifting the surface between multiple mechanically stable states.The mat can remain flat, fold into inward-facing contours for face-to-face seating, or curve unidirectionally to support parallel sitting configurations.

Each bistable unit retains its deformed shape without continuous energy input, allowing persistent configuration without the need for actuators or external control systems. This passive, mechanically programmable system offers a lightweight and scalable alternative to conventional adaptive surfaces. It can be reconfigured

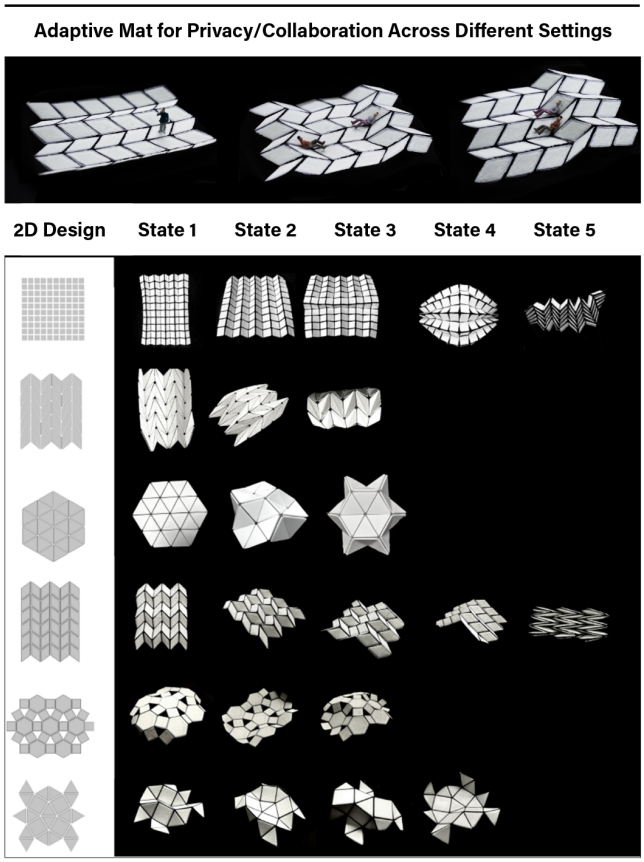

Figure 14: (Top) Shape-changing mat: a responsive surface for interactions ranging from private to public. (Bottom) A chart of tessellations—identical regular polygons, semi-regular patterns, and polymorphic tessellations—showing their resulting morphologies and number of stable states.

into functional topographies—such as backrests, raised platforms for tools or meals, or ergonomic contours for resting—based entirely on material-level design.

To explore the design space, we investigated regular, semi-regular, and polymorphic tessellation strategies. Regular tessellations, composed of a single polygon type (e.g., triangles, squares, or hexagons), exhibit uniform mechanical behavior and bistability. Square grids support orthogonal snapping, triangular grids favor diagonal folding, and hexagonal arrangements enable globally continuous deformation. Semi-regular tessellations extend this behavior by combining polygon types while maintaining consistent vertex configurations (e.g., alternating triangles and hexagons), supporting spatially varied morphing. Polymorphic tessellations introduce irregular combinations of regular polygons, enabling localized tuning of bistability and region-specific functionality within a single textile.

This approach supports the development of responsive furniture, deployable structures, and architectural textiles that reshape in response to real-time input—such as body pressure, environmental triggers, or embedded sensor feedback—integrating input, structure, and morphological response within a unified material platform.

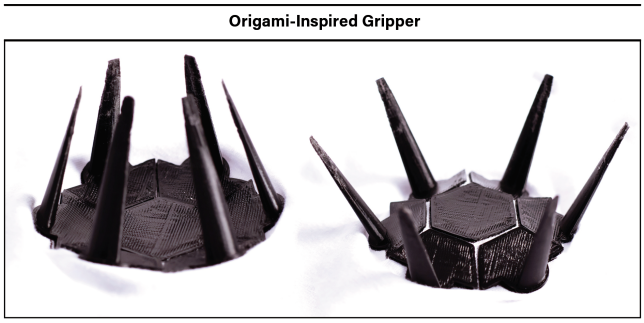

Figure 15: Origami-Inspired Gripper Demonstrating Tactile, Passive Capture of Objects.

5.6 Origami-Inspired Grabbing Mechanism: Tactile, Passive Object Capture

Drawing inspiration from origami-based folding mechanics, we developed a passive gripper system capable of contact-driven actuation through programmable mechanical instabilities (Figure 15). The design leverages a tessellated array of bistable hexagonal units, each engineered to transition between flat and curled configurations in response to localized mechanical forces—such as the weight of an object, finger pressure, or incidental touch—without requiring motors, sensors, or external energy input. Upon contact with lightweight items (e.g., a coin, a small tool, or a falling leaf), individual units undergo snap-through instability, curling inward to capture and hold the object through passive enclosure. This bistability also functions as an energy-absorbing mechanism, helping to protect falling objects from impact.

This bistable transformation not only enables mechanical locking but also allows the structure to store and maintain elastic energy within its geometric framework. Once actuated, the gripper remains in its deformed state until manually reset, eliminating the need for continuous energy supply or active control systems. By tuning pixel scale, geometry, and spacing, the sensitivity and responsiveness of the grip can be modulated, supporting customized interactions for different object sizes and contact scenarios. This material-centric approach emphasizes embodied interaction, wherein the interface behavior emerges directly from its structural design and physical configuration. this also behaves like energy absorbing protecting falling object.

6 Discussion

This study introduces PixBric, a programmable morphing platform that leverages bistable, pixel-based geometries printed onto biaxially pre-stretched fabrics to achieve controlled, reversible shape transformations. By precisely tuning geometric parameters such as inter-pixel spacing, scale, and thickness, PixBric enables a form of geometric actuation that supports spatially programmable deformation patterns—ranging from discrete snapping units to globally coordinated curvature. This system bridges the scale from microstructures such as bistable rings to macro-scale adaptive surfaces such as shape-changing mats and reconfigurable textiles.

Our experimental results identified optimal design parameters that maximize morphing fidelity and bistability. Specifically, pixel

widths and thicknesses between 0.5–2mm exhibited the strongest snap-through behavior, consistent curvature, and repeatable shape retention without excessive stiffness or material fatigue. In addition, the morphology of each tessellated unit critically influenced mechanical behavior. Triangular and rectangular geometries promoted edge-aligned snapping, supporting directional morphing, while hexagonal tessellations facilitated smooth, isotropic deformation across surfaces due to their three-edge vertex topology and efficient space-filling.

Despite its versatility, PixBric currently faces limitations in scalability. Fabrication via FDM 3D printing restricts both the surface area and resolution of deployable designs. Future efforts should explore scalable, continuous fabrication methods such as roll-to-roll additive manufacturing, screen printing of thermoplastics, or stencil-based deposition techniques to improve production speed and expand the size of morphing interfaces. These methods could support the creation of meter-scale deployable morphing textiles, opening pathways toward applications in architecture, furniture, or soft robotics. Additionally, advances in multi-material extrusion and robotic printing systems may allow for the seamless integration of structural and responsive elements across large surfaces.

Third, the interaction affordances and user experience of shape-morphing textiles remain underexplored. While this work demonstrates programmable structural transitions and morphing behavior, real-world deployment—particularly in wearables, furniture, or tactile interfaces—demands evaluation of comfort, durability, reversibility under repeated use, and intuitiveness of interaction. Investigating how users perceive, manipulate, and interpret these morphing behaviors is critical to refining the functional language of bistable materials. Longitudinal user studies and participatory design approaches could reveal new affordances, co-opted uses, and design patterns that were not anticipated in initial prototyping.

Lastly, from a theoretical perspective, this work contributes to an emerging understanding of material computation, wherein physical structure encodes not just form but dynamic function. However, we have not yet formalized computational frameworks to model, predict, and optimize morphing behaviors across complex tessellation patterns. Future work could incorporate finite element modeling, graph-based tessellation analysis, or machine-learning-driven design optimization to extend the design space and automate performance tuning. Furthermore, integrating feedback mechanisms—such as embedded sensors—would enable closed-loop systems capable of self-adjusting shape states based on real-time sensing and interaction.

In summary, PixBric provides a strong foundation for reconfigurable material systems, yet its broader adoption will depend on overcoming challenges of scale, material integration, and user experience. For TEI practitioners, PixBric serves as both a research framework and a practical prototyping tool—its simulation–fabrication pipeline enables designers, educators, and interaction researchers to explore programmable morphology without requiring advanced mechanical expertise. Continued development of fabrication, simulation, and evaluation methods in parallel will be essential to fully realize the potential of programmable morphing textiles in interactive environments, embodied interfaces, and responsive architectural applications.

7 Conclusion

PixBric embodies the theme of *Tide + Tied* by weaving together computational design and textile-based material intelligence—uniting the flowing potential of digital simulation and fabrication with the grounded constraints of elasticity and bistability. It introduces a cross-disciplinary language of shape change that is simultaneously rigorous in its engineering foundations, expressive in form, tangible in interaction, and accessible in fabrication. Therefore, for HCI and TEI researchers, this framework extends the understanding of tangible structural formation through pixel-level precision and computational simulation. For material scientists, it offers a more rigorous insight into the reversible shape morphing of 3D-printed structures on pre-stretched fabrics, achieved through variations in geometry and spacing. It demonstrates the potential of structural geometry to serve as both the medium and mechanism for interactive, morphable behaviors.

Acknowledgments

We would like to thank Yue Yang for her invaluable assistance in developing the cloud-based Human UI interface. We also acknowledge the support provided through the LEGO Papert Fellowship. This research was supported by the National Research Foundation of Korea (NRF) grant funded by the Korea government (MSIT) (RS-2025-16902996).

References

[1] Asterios Agkathidis, Yannis Berdos, and Adam Brown. 2018. Active Membranes: 3D Printing of Elastic Fibre Patterns on Pre-Stretched Textiles. *International Journal of Architectural Computing* 17, 1 (2018), 74–87. doi:10.1177/1478077118800890

[2] Yoseph Bar-Cohen. 2004. Electroactive polymer (EAP) actuators as artificial muscles: reality, potential, and challenges. *Proceedings of the SPIE Smart Structures and Materials 2004: Electroactive Polymer Actuators and Devices (EAPAD)* 5385 (2004), 1–7. doi:10.1117/12.538157

[3] Simone Battisti, Daniel Calegaro, Paolo Marcandelli, Alice Todeschini, and Stefano Mariani. 2024. Learning the Buckled Geometry of 3D Printed Stiffeners of Pre-Stretched Soft Membranes. *Engineering Proceedings* 72, 1 (2024), 3. doi:10.3390/engproc72010003

[4] Katia Bertoldi, Pedro M. Reis, Stephen Willshaw, and Tom Mullin. 2010. Negative Poisson's ratio behavior induced by an elastic instability. *Advanced Materials* 22, 3 (2010), 361–366. doi:10.1002/adma.200901956

[5] Bryan Bishop-Moser and Sridhar Kota. 2015. Design and modeling of a pneumatically actuated peristaltic micropump. *IEEE/ASME Transactions on Mechatronics* 20, 6 (2015), 2766–2773. doi:10.1109/TMECH.2015.2400214

[6] Marcelo Coelho and Jamie Zigelbaum. 2011. Shape-Changing Interfaces. *Personal and Ubiquitous Computing* 15, 2 (2011), 161–173. doi:10.1007/s00779-010-0311-y

[7] Jawaid Daudpoto Dileep Kumar and Bhawani Shankar Chowdhry. 2020. Challenges for practical applications of shape memory alloy actuators. *Materials Research Express* (2020). doi:10.1088/2053-1591/aba403

[8] Sean Follmer, Daniel Leithinger, Alex Olwal, Nadia Cheng, and Hiroshi Ishii. 2013. inFORM: Dynamic Physical Affordances and Constraints through Shape and Object Actuation. In *Proceedings of the 26th Annual ACM Symposium on User Interface Software and Technology (UIST '13)*. Association for Computing Machinery, 417–426. doi:10.1145/2501988.2502032

[9] A. S. Gladman, E. A. Matsumoto, R. G. Nuzzo, L. Mahadevan, and J. A. Lewis. 2016. Biomimetic 4D printing. *Nature Materials* 15, 4 (2016), 413–418. doi:10.1038/nmat4544

[10] Lorenzo Guiducci, Agata Kycia, Christiane Sauer, and Peter Fratzl. 2022. Self-organized rod undulations on pre-stretched textiles. *Bioinspiration & Biomimetics* 17, 3 (2022), 036007. doi:10.1088/1748-3190/ac5b85

[11] Ruslan Guseinov, Connor McMahan, Jesús Pérez, Chiara Daraio, and Bernd Bickel. 2020. Programming temporal morphing of self-actuated shells. *Nature Communications* 11 (2020), 237. doi:10.1038/s41467-019-14015-2

[12] Ruslan Guseinov, Eder Miguel, and Bernd Bickel. 2017. CurveUps: shaping objects from flat plates with tension-actuated curvature. *ACM Transactions on Graphics (TOG)* 36, 4 (2017), 64:1–64:12. doi:10.1145/3072959.3073709

[13] Lars Erik Holmquist, Johan Redström, and Peter Ljungstrand. 1999. Bricks: Laying the foundations for graspable user interfaces. In *Proceedings of the SIGCHI*

Conference on Human Factors in Computing Systems. ACM, 442–449. doi:10.1145/223904.223964

[14] Filip Ilievski, Aaron D. Mazzeo, Robert F. Shepherd, Xiaonan Chen, and George M. Whitesides. 2011. Soft robotics for chemists. *Angewandte Chemie International Edition* 50, 8 (2011), 1890–1895. doi:10.1002/anie.201006464

[15] Hiroshi Ishii. 2008. Tangible user interfaces. *ACM Queue* 6, 5 (2008), 33–37. doi:10.1145/1391289.1391308

[16] Yu Jiang, Alice C Haynes, Narjes Pourjafarian, Jan Borchers, and Jürgen Steimle. 2024. Embrogami: Shape-Changing Textiles with Machine Embroidery. In *Proceedings of the 37th Annual ACM Symposium on User Interface Software and Technology* (Pittsburgh, PA, USA) *(UIST '24)*. Association for Computing Machinery, New York, NY, USA, Article 63, 15 pages. doi:10.1145/3654777.3676431

[17] David Jourdan, Melina Skouras, Etienne Vouga, and Adrien Bousseau. 2020. Printing-on-Fabric Meta-Material for Self-Shaping Architectural Models. https://ethz.ch/content/dam/ethz/special-interest/arch/iaa/institute-dam/documents/AAG2020-Proceedings.pdf Presented at Advances in Architectural Geometry 2020, ETH Zurich.

[18] Sangbae Kim, Cecilia Laschi, and Barry Trimmer. 2013. Soft robotics: a bioinspired evolution in robotics. *Trends in Biotechnology* 31, 5 (2013), 287–294. doi:10.1016/j.tibtech.2013.03.002

[19] Yael Klein, Efi Efrati, and Eran Sharon. 2007. Shaping of elastic sheets by prescription of non-Euclidean metrics. *Science* 315, 5815 (2007), 1116–1120. doi:10.1126/science.1135994

[20] Cecilia Laschi and Matteo Cianchetti. 2016. Soft robotics: Trends, applications and challenges. *Robotics and Autonomous Systems* 80 (2016), 3–15.

[21] Y. Liu, J. Genzer, and M. D. Dickey. 2016. "2D or not 2D": Shape-programming polymer sheets. *Progress in Polymer Science* 52 (2016), 79–106. doi:10.1016/j.progpolymsci.2015.09.001

[22] Nan Ma and Gangbing Song. 2010. Shape memory alloy actuators: Design challenges and solutions. *Smart Materials and Structures* 19, 12 (2010), 123001. doi:10.1088/0964-1726/19/12/123001

[23] Carmel Majidi. 2014. Soft robotics: a perspective—current trends and prospects for the future. *Soft Robotics* 1, 1 (2014), 5–11. doi:10.1089/soro.2013.0001

[24] Achim Menges. 2012. Material computation: Higher integration in morphogenetic design. *Architectural Design* 82, 2 (2012), 14–21. doi:10.1002/ad.1371

[25] Farhang Momeni, Nazanin S. Hassani, Xiaoying Liu, and Jun Ni. 2017. A Review of 4D Printing. *Materials & Design* 122 (2017), 42–79. doi:10.1016/j.matdes.2017.02.068

[26] Ken Nakagaki, Takashi Nitta, and Hiroshi Ishii. 2015. LineFORM: Actuated Curve Interfaces for Display, Interaction, and Constraint. In *Proceedings of the 28th Annual ACM Symposium on User Interface Software and Technology (UIST '15)*. Association for Computing Machinery, 333–339. doi:10.1145/2807442.2807452

[27] Jifei Ou, Lining Yao, David Tauber, Jürgen Steimle, and Hiroshi Ishii. 2016. bioLogic: Natto Cells as Nanoactuators for Shape Changing Interfaces. In *Proceedings of the 2016 CHI Conference on Human Factors in Computing Systems (CHI '16)*. Association for Computing Machinery, 3745–3756. doi:10.1145/2858036.2858443

[28] Jifei Ou, Lining Yao, David Tauber, Jürgen Steimle, Ryuma Niiyama, and Hiroshi Ishii. 2014. jamSheets: Thin Interfaces with Tunable Stiffness Enabled by Layer Jamming. In *Proceedings of the 8th International Conference on Tangible, Embedded, and Embodied Interaction (TEI '14)*. Association for Computing Machinery, 65–72. doi:10.1145/2540930.2540971

[29] Johannes T. B. Overvelde, Shengtian Shan, and Katia Bertoldi. 2012. Compaction through buckling in 2D periodic, soft and porous structures: Effect of pore shape. *Advanced Materials* 24, 17 (2012), 2337–2342. doi:10.1002/adma.201200210

[30] Ron Pelrine, Roy Kornbluh, Qibing Pei, and Joseph Joseph. 2000. High-speed electrically actuated elastomers with strain greater than 100%. *Science* 287, 5454 (2000), 836–839. doi:10.1126/science.287.5454.836

[31] Brady Peters and Vanessa Vasquez. 2013. Architectural materialization of environmentally responsive shape-change. In *Proceedings of the Symposium on Simulation for Architecture and Urban Design*. 1–8. doi:10.1145/2504488.2504503

[32] Matteo Pezzulla, Gabriel Smith, Paola Nardinocchi, and Douglas P. Holmes. 2017. Geometry and mechanics of thin growing bilayers. *Soft Matter* 13, 36 (2017), 9230–9236. doi:10.1039/C7SM01738A

[33] Isabel P. S. Qamar, Rainer Groh, David Holman, and Anne Roudaut. 2018. HCI meets Material Science: A Literature Review of Morphing Materials for the Design of Shape-Changing Interfaces. In *Proceedings of the 2018 CHI Conference on Human Factors in Computing Systems*. ACM, 1–23. doi:10.1145/3173574.3173948

[34] Michael L. Rivera, Melissa Moukperian, Daniel Ashbrook, Jennifer Mankoff, and Scott E. Hudson. 2017. Stretching the Bounds of 3D Printing with Embedded Textiles. In *Proceedings of the 2017 CHI Conference on Human Factors in Computing Systems* (Denver, Colorado, USA) *(CHI '17)*. Association for Computing Machinery, New York, NY, USA, 497–508. doi:10.1145/3025453.3025460

[35] Daniela Rus and Michael T. Tolley. 2015. Design, fabrication and control of soft robots. *Nature* 521, 7553 (2015), 467–475. doi:10.1038/nature14543

[36] Timothy C. Shyu, Pablo F. Damasceno, Peter M. Dodd, Aaron Lamoureux, Lijie Xu, Mark Shlian, Max Shtein, Sharon C. Glotzer, and Nicholas A. Kotov. 2015. A kirigami approach to engineering elasticity in nanocomposites through patterned defects. *Nature Materials* 14 (2015), 785–789. doi:10.1038/nmat4327

[37] Lingyun Sun, Ziqian Shao, Danli Luo, Jianzhe Gu, Ye Tao, Lining Yao, and Guanyun Wang. 2020. FabricFit: Transforming Form-Fitting Fabrics. In *Adjunct Proceedings of the 33rd Annual ACM Symposium on User Interface Software and Technology*. ACM, 99–101. doi:10.1145/3379350.3416198

[38] Ami Takahashi, Yu Soma, Karin Tomonaga, and Hiroki Sato. 2024. Flexmock: Fast, easy, stockable smocking method using 3D printed self-shrinkable pattern sheet. In *Adjunct Proceedings of the 37th Annual ACM Symposium on User Interface Software and Technology*. 1–3.

[39] Lining Yao, Zhiyuan Liu, Jifei Ou, Nicole Cheng, Xuanhe Wang, and Hiroshi Ishii. 2013. Printed Paper Actuators: Fabrication and Analysis of Thermally-Actuated Structures Made from Paper. In *Proceedings of the 26th Annual ACM Symposium on User Interface Software and Technology (UIIST '13)*. Association for Computing Machinery, 229–238.

[40] Lining Yao, Ryuma Niiyama, Jifei Ou, Sean Follmer, Clark Della Silva, and Hiroshi Ishii. 2013. PneUI: Pneumatically Actuated Soft Composite Materials for Shape Changing Interfaces. In *Proceedings of the 26th Annual ACM Symposium on User Interface Software and Technology (UIST '13)*. Association for Computing Machinery, 13–22. doi:10.1145/2501988.2502037

[41] Lining Yao, Jifei Ou, Chin-Yi Cheng, Wen Wang, Yao-Wen Hsu, and Hiroshi Ishii. 2015. bioLogic: Natto Cells as Nano-Actuators for Shape Changing Interfaces. In *Proceedings of the 33rd Annual ACM Conference on Human Factors in Computing Systems (CHI '15)*. Association for Computing Machinery, 1–10. doi:10.1145/2702123.2702611

[42] Lining Yao, Jesse Ou, Nicole Cheng, Henry Steiner, Xuanhe Wang, and Hiroshi Ishii. 2015. PneUI: pneumatically actuated soft composite materials for shape changing interfaces. In *Proceedings of the 33rd Annual ACM Conference on Human Factors in Computing Systems (CHI '15)*. ACM, 4381–4390. doi:10.1145/2702123.2702617

[43] Lining Yao, Jifei Ou, Nicole Cheng, Xuanhe Wang, and Hiroshi Ishii. 2017. Breathing, Growing, and Self-Transforming Matter: Natural and Artificial Biological Materials for Shape-Changing Interfaces. *Journal of Polymer Science Part B: Polymer Physics* 55, 9 (2017), 691–700. doi:10.1002/polb.24337

[44] Lining Yao, Jifei Ou, and Hiroshi Ishii. 2016. Transflux: A Feedback-Driven Programmable Matter System for Design Exploration. In *Proceedings of the 2016 ACM Conference on Designing Interactive Systems (DIS '16)*. Association for Computing Machinery, 1096–1107. doi:10.1145/2901790.2901863

[45] Hyejun Youn. 2021. AuxeticBreath: Changing Perception of Respiration. In *Proceedings of the Fifteenth International Conference on Tangible, Embedded, and Embodied Interaction (TEI '21)*. Association for Computing Machinery, New York, NY, USA. doi:10.1145/3430524.3444636 Art/installation presented at TEI '21; Red Dot Design Concept Winner and A'Design Award Honoree..

[46] Hye Jun Youn and Ali Shtarbanov. 2022. PneuBots: Modular Inflatables for Playful Exploration of Soft Robotics. In *Extended Abstracts of the 2022 CHI Conference on Human Factors in Computing Systems (CHI EA '22)*. Association for Computing Machinery. doi:10.1145/3491101.3514490

[47] M. Zarek, M. Layani, I. Cooperstein, E. Sachyani, D. Cohn, and S. Magdassi. 2016. 3D Printing of Shape Memory Polymers for Flexible and One-Time Actuated Devices. *Advanced Materials* 28, 22 (2016), 4449–4454. doi:10.1002/adma.201504597

[48] X. Zheng et al. 2012. Programming buckling in mechanical metamaterials. *Nature Communications* 3 (2012), 1110. doi:10.1038/ncomms2122